The Action of Red Light on Solid Caryophyllene Nitrosite, $C_{15}H_{24}N_2O_3$: (*i*) the Reaction Products; (*ii*) the Crystal Structures of Caryophyllene Nitrosite and of Dinitrocaryophyllene, $C_{15}H_{24}N_2O_4$; (*iii*) Electron Paramagnetic Resonance Studies; and (*iv*) the Solid-state Reaction Mechanisms

Andrew A. Freer, Derek K. MacAlpine, Judith A. Peacock, and Andrew L. Porte *
Department of Chemistry, The University of Glasgow, Glasgow G12 8QQ

The stereochemistries of caryophyllene nitrosite (**3**) and dinitrocaryophyllene (**5**) have been determined by *X*-ray analyses of their crystal structures. Crystallographic data are: caryophyllene nitrosite, a = 6.476(4), b = 13.199(2), c = 18.784(2) Å, Z = 4, space group $P2_12_12_1$; dinitrocaryophyllene, a = 6.405(4), b = 12.991(2), c = 9.797(3) Å, β = 93.04(4)°, Z = 2, space group $P2_1$. The molecular conformations are very similar and caryophyllene nitrosite forms solid solutions in dinitrocaryophyllene. Irradiation of these solid solutions with red light generates a monoalkyl nitroxide radical (**11**), in two symmetry-related orientations, whose spin-Hamiltonian parameters and orientations in the unit cell of the dinitrocaryophyllene crystal have been determined by detailed analyses of single-crystal e.p.r. spectra. Photolysis of pure solid caryophyllene nitrosite with red light generates N_2, NO, NO_2, dinitrocaryophyllene (**5**), nitro-nitratocaryophyllene (**7**), isocaryophyllene (**6**), and 4,8-bismethylene-11,11-dimethyl-5-nitrobicyclo[7.2.0]undecane (**8**) and its isomers, compounds (**9**) and (**10**). Three nitroxide radicals, two of which have been identified as compounds (**11**) and (**15**) are also generated. The combination of chemical, *X*-ray, and spectroscopic evidence enables the steps in the solid photolysis reactions to be unravelled.

The history of the chemistry of caryophyllene, one of the major components of oil of cloves, and of its many rearrangement products, has been one of triumphant collaboration between organic chemistry and *X*-ray crystallography.[1] The structure of the parent hydrocarbon and its absolute stereochemistry, (**1**), were assigned (*a*) from the results obtained from intensive chemical degradation studies carried out by Barton[2–5] and Sǒrm[6,7] and their co-workers; (*b*) from measurements of the molecular rotations of tricyclic derivatives of established stereochemistry;[8] and (*c*) from *X*-ray analyses of several derivatives.[1] Structure (**1**) was later confirmed by the total synthesis of (±)-caryophyllene[9] and by *X*-ray analysis of the 'iodonitrosite' derivative, the nitroxide radical (**2**),[10,11] that is obtained when caryophyllene nitrosite reacts with iodine. Structure (**2**) for the 'iodonitrosite' requires the structure and stereochemistry of caryophyllene nitrosite to be as shown in (**3**).[10,11]

Caryophyllene nitrosite was first synthesized in 1898,[12] and for many years it was used to characterize caryophyllene. It absorbs at 270 nm and in the red region of the spectrum, at 670 nm, this latter transition, the π* ← n transition of the nitroso group, being responsible for the deep blue colour of the solid. It has been known for a long time that caryophyllene nitrosite solutions are photolysed by red light and that the nature of the photolysis products is solvent dependent.[13–22] When the blue solid is red-irradiated in the absence of air, it decomposes to a yellow viscous liquid, and preliminary studies show that the products of photolysis include nitrogen, nitric oxide, nitrogen dioxide,[22] and the nitroxide radical (**4**).[23]

We have carried out several studies in connection with the red photolysis of solid caryophyllene nitrosite including: (*i*) more detailed examination of the diamagnetic products of the photolysis reactions; (*ii*) single-crystal *X*-ray analyses of caryophyllene nitrosite and dinitrocaryophyllene; (*iii*) single-crystal e.p.r. studies of the radical obtained when dinitrocaryophyllene doped with caryophyllene nitrosite is red-irradiated; and (*iv*) polycrystalline e.p.r. studies of the radicals that are formed when solid caryophyllene nitrosite is exhaustively irradiated with red light.

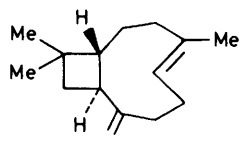

(**1**)

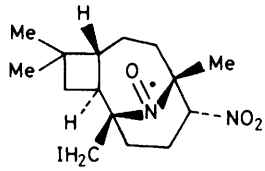

(**2**)

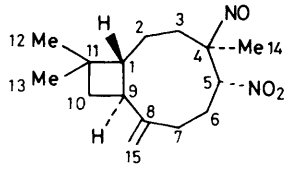

(**3**)

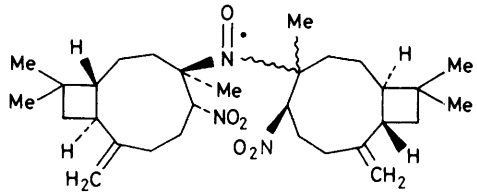

(**4**)

The results of these studies, described in this paper, enable us to unravel the sequence of solid-state reactions that take place when crystals of caryophyllene nitrosite are irradiated with red light.

Results and Discussion

(*i*) *The Diagmagnetic Products of the Photochemical Reactions.*—Caryophyllene nitrosite is obtained by allowing

Table 1.

Band	R_F value	Appearance	M.p. (from ethanol) (°C)
A	0.64	Blue needles	116 ± 1
B	0.59	Colourless needles	127 ± 0.5

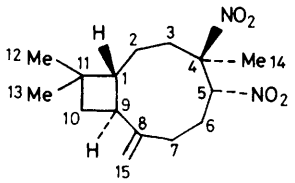

(5)

caryophyllene to react in the dark with an equivalent amount of N_2O_3 generated by dropwise addition of glacial acetic acid to a saturated aqueous solution of sodium nitrite.[12,13] Blue crystals and a yellow oil are obtained from this reaction. Recrystallization of the blue crystals from ethanol followed by chromatography on silica plates using ether–light petroleum (1:1) as eluant reveals the presence of two components whose characteristics are listed in Table 1. Elemental analysis, n.m.r., i.r., and mass spectra show that substance A is caryophyllene nitrosite (**3**), and substance B is dinitrocaryophyllene (**5**). The spectroscopic properties of these compounds are so similar that their configurations and conformations must be very similar. Caryophyllene nitrosite forms solid solutions in dinitrocaryophyllene.

The non-gaseous photolysis products obtained when pure, solid, caryophyllene nitrosite is exhaustively red-irradiated can be separated into two fractions. The first of these is soluble in light petroleum (b.p. 40—60 °C) and contains only diamagnetic species: this fraction contains the more abundant photolysis products. The second fraction is insoluble in this mixed solvent, and it is paramagnetic, although it is magnetically dilute: it contains several nitroxide radicals. Isocaryophyllene (**6**), crystals of dinitrocaryophyllene, crystals of nitro-nitratocaryophyllene (**7**), and an oil containing several olefins can be isolated from the soluble fraction. We have not managed to separate and purify these olefins but i.r. and n.m.r. evidence shows that the mixture consists of (**8**) and smaller amounts of its isomers (**9**) and (**10**).

(ii) The Crystal Structures of Caryophyllene Nitrosite and of Dinitrocaryophyllene.—Crystal data for caryophyllene nitrosite (**3**). $C_{15}H_{24}N_2O_3$, M = 280.4, orthorhombic, a = 6.476(4), b = 13.199(2), c = 18.784(2) Å, U = 1 605.6 Å^3, $F(000)$ = 608, Z = 4, D_c = 1.16 g cm^{-3}, μ(Mo-K_α) = 0.87 cm^{-1}, space group $P2_12_12_1$.

Crystal data for dinitrocaryophyllene (**5**). $C_{15}H_{24}N_2O_4$, M = 296.4, monoclinic, a = 6.405(4), b = 12.991(2), c = 9.797(3) Å, β = 93.04(4)°, U = 814.0 Å^3, $F(000)$ = 320, Z = 2, D_c = 1.21 g cm^{-3}, μ(Mo-K_α) = 0.95 cm^{-1}, space group $P2_1$.

1 834 and 2 188 independent reflections were collected for caryophyllene nitrosite and dinitrocaryophyllene, respectively, on an Enraf–Nonius CAD4 X-ray diffractometer. The crystal structure of the dinitro derivative was elucidated by straightforward application of MULTAN,[24] but several difficulties were encountered in the analysis of the nitrosite, and the program MITHRIL[25] was used to determine its crystal structure. Normalization using Wilson plot statistics produced one large E-magnitude, E_{041} = 3.61, compared with 2.77 for the next. Renormalizing the data using the K-curve method altered

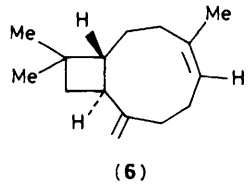

(6)

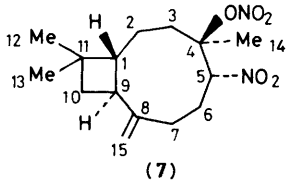

(7)

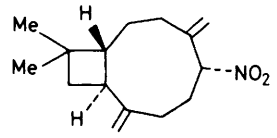

(8)

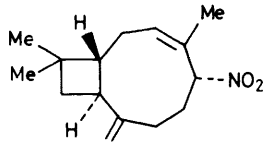

(9)

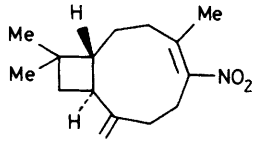

(10)

these to 3.35 and 3.01, respectively. Σ_2 and convergence gave rise to an apparent abundance of relationships, along with a good starting set, but tangent refinement was inconclusive and the figures of merit were inconsistent. Negative quartets were therefore generated for the top 100 E-magnitudes, but although this brought about some improvement, the problem with the figures of merit still persisted. Examination of the convergence procedures showed that the quartet invariants were dominating the phase-determining procedures at this stage, and so in order to obtain a better balance between triplet and quartet participation in convergence the number of reflections used to generate quartets was confined to 60 reflections with the largest E-magnitudes. The Hull–Irwin[26] statistically weighted tangent formula was used instead of the usual weighting scheme.

The atomic and thermal parameters subsequently refined to final R values of 0.085 and 0.036 (R_w = 0.121 and 0.044) for caryophyllene nitrosite and dinitrocaryophyllene, respectively, for 714 and 1 453 reflections [$I \geqslant 2.5\sigma(I)$]. Because of the smaller number of useful reflections, hydrogen atoms were only included in the structure factor part of the final least-squares calculation in the nitrosite. For the nitrosite, 181 parameters were refined. In the case of the dinitro derivative, 286 parameters were refined.

Bond lengths in the two molecules are compared in Table 2, bond angles in Table 3, and torsion angles in Table 4. Atomic coordinates are given in Table 5. Observed and calculated structure factors and thermal parameters are available as Supplementary data.* The conformations of the molecules are shown in Figure 1, and stereo views of the crystal structures are shown in Figures 2 and 3. Although these compounds are not isomorphous the molecular conformations and packing within the two crystal structures are so very similar that it is not surprising that caryophyllene nitrosite is so easily doped into the dinitrocaryophyllene crystal structure.

* Supplementary data available (No. SUP 56213, 13 pp.): atomic coordinates and thermal parameters for the two compounds. See Instructions for Authors, section 4.0 (January issue). Structure factors are available from the editorial office on request.

Table 2. Bond lengths (Å) in dinitrocaryophyllene and caryophyllene nitrosite

Bond	Compound	
	Dinitrocaryophyllene	Caryophyllene nitrosite
O(1)–N(1)	1.210(5)	1.10(2)
O(2)–N(1)	1.199(5)	
O(3)–N(2)	1.210(6)	1.23(2)
O(4)–N(2)	1.201(6)	1.18(2)
N(1)–C(4)	1.562(5)	1.65(3)
N(2)–C(5)	1.512(6)	1.58(2)
C(1)–C(2)	1.532(5)	1.50(2)
C(1)–C(9)	1.568(5)	1.57(2)
C(1)–C(11)	1.561(5)	1.49(2)
C(2)–C(3)	1.532(6)	1.54(2)
C(3)–C(4)	1.537(7)	1.57(2)
C(4)–C(5)	1.531(6)	1.48(2)
C(4)–C(14)	1.508(6)	1.55(3)
C(5)–C(6)	1.533(6)	1.53(2)
C(6)–C(7)	1.523(6)	1.51(2)
C(7)–C(8)	1.500(7)	1.54(2)
C(8)–C(9)	1.497(6)	1.50(2)
C(8)–C(15)	1.318(6)	1.30(2)
C(9)–C(10)	1.541(7)	1.53(2)
C(10)–C(11)	1.530(7)	1.54(2)
C(11)–C(12)	1.519(6)	1.52(3)
C(11)–C(13)	1.509(8)	1.55(3)

Table 3. Bond angles (°) in dinitrocaryophyllene and caryophyllene nitrosite

Angle	Compound	
	Dinitrocaryophyllene	Caryophyllene nitrosite
O(1)–N(1)–O(2)	124.3(4)	
O(1)–N(1)–C(4)	116.8(3)	103(2)
O(2)–N(1)–C(4)	118.6(4)	
O(3)–N(2)–O(4)	124.9(5)	127(1)
O(3)–N(2)–C(5)	116.6(4)	116(1)
O(4)–N(2)–C(5)	118.3(4)	116(1)
C(2)–C(1)–C(9)	123.7(3)	125(1)
C(2)–C(1)–C(11)	118.1(3)	120(1)
C(9)–C(1)–C(11)	88.6(3)	90(1)
C(1)–C(2)–C(3)	117.3(4)	118(1)
C(2)–C(3)–C(4)	120.3(4)	121(1)
N(1)–C(4)–C(3)	102.2(4)	100(1)
N(1)–C(4)–C(5)	107.5(3)	100(1)
N(1)–C(4)–C(14)	108.8(3)	118(1)
C(3)–C(4)–C(5)	109.9(3)	110(1)
C(3)–C(4)–C(14)	112.5(4)	112(1)
C(5)–C(4)–C(14)	115.1(5)	114(1)
N(2)–C(5)–C(4)	112.6(3)	111(1)
N(2)–C(5)–C(6)	106.5(4)	106(1)
C(4)–C(5)–C(6)	113.5(3)	118(1)
C(5)–C(6)–C(7)	113.7(4)	114(1)
C(6)–C(7)–C(8)	112.7(4)	113(1)
C(7)–C(8)–C(9)	116.5(4)	113(1)
C(7)–C(8)–C(15)	120.0(5)	120(1)
C(9)–C(8)–C(15)	123.5(5)	126(1)
C(1)–C(9)–C(8)	120.2(3)	120(1)
C(1)–C(9)–C(10)	87.0(4)	86(1)
C(8)–C(9)–C(10)	120.3(4)	119(1)
C(9)–C(10)–C(11)	90.8(3)	90(1)
C(1)–C(11)–C(10)	87.5(3)	88(1)
C(1)–C(11)–C(12)	113.3(4)	119(1)
C(1)–C(11)–C(13)	114.9(4)	114(1)
C(10)–C(11)–C(12)	111.3(5)	108(1)
C(10)–C(11)–C(13)	118.2(4)	117(1)
C(12)–C(11)–C(13)	110.0(5)	109(1)

Table 4. Torsion angles (°) in dinitrocaryophyllene and caryophyllene nitrosite

Torsion angle	Compound	
	Dinitrocaryophyllene	Caryophyllene nitrosite
(*a*) 9-Membered ring		
C(9)–C(1)–C(2)–C(3)	−107.9(5)	−101(2)
C(2)–C(1)–C(9)–C(8)	94.7(5)	92(1)
C(1)–C(2)–C(3)–C(4)	86.8(5)	90(1)
C(2)–C(3)–C(4)–C(5)	−55.4(4)	−58(1)
C(3)–C(4)–C(5)–C(6)	90.4(4)	89(1)
C(4)–C(5)–C(6)–C(7)	−154.9(5)	−152(2)
C(5)–C(6)–C(7)–C(8)	60.4(4)	60(1)
C(6)–C(7)–C(8)–C(9)	47.6(4)	51(1)
C(7)–C(8)–C(9)–C(1)	−94.7(5)	−101(1)
(*b*) 4-Membered ring		
C(11)–C(1)–C(9)–C(10)	−18.3(3)	−18(1)
C(11)–C(10)–C(9)–C(1)	18.7(3)	17(7)
O(1)–N(1)–C(4)–C(3)	77.1(5)	−84(1)
O(2)–N(1)–C(4)–C(3)	−97.1(5)	
O(1)–N(1)–C(4)–C(5)	−38.5(4)	
O(2)–N(1)–C(4)–C(5)	147.2(5)	163(2)
O(3)–N(2)–C(5)–C(4)	141.0(6)	132(2)
O(4)–N(2)–C(5)–C(4)	−42.8(5)	−55(1)
O(3)–N(2)–C(5)–C(6)	−93.9(5)	−99(1)
O(4)–N(2)–C(5)–C(6)	82.4(5)	74(1)

Table 5. Atomic co-ordinates

Caryophyllene nitrosite

	x/a	*y/b*	*z/c*	*U*
O(1)	−0.945(3)	0.073(1)	−0.171(1)	0.17(1)
O(3)	−1.102 5(15)	−0.190 9(10)	−0.292 2(7)	0.12(1)
O(4)	−0.943 1(19)	−0.196 5(9)	−0.191 3(5)	0.13(1)
N(1)	−0.968 (3)	0.024(1)	−0.218(1)	0.12(1)
N(2)	−0.963 9(19)	−0.168 2(8)	−0.250 3(6)	0.086(9)
C(1)	−0.488 4(18)	0.026 8(8)	−0.404 4(6)	0.053(7)
C(2)	−0.458(2)	0.063(1)	−0.329(1)	0.073(9)
C(3)	−0.651(2)	0.075(1)	−0.282(1)	0.08(1)
C(4)	−0.732(2)	−0.016(1)	−0.236(1)	0.07(1)
C(5)	−0.779(2)	−0.104(1)	−0.282(1)	0.060(8)
C(6)	−0.605 3(18)	−0.180 0(10)	−0.297 3(6)	0.055(8)
C(7)	−0.627(2)	−0.233(1)	−0.368(1)	0.07(1)
C(8)	−0.629(2)	−0.159(1)	−0.431(1)	0.065(8)
C(9)	−0.452 2(18)	−0.084 9(9)	−0.430 7(5)	0.050(7)
C(10)	−0.381(2)	−0.037(1)	−0.500(1)	0.080(9)
C(11)	−0.352(2)	0.065(1)	−0.462(1)	0.068(9)
C(12)	−0.417(3)	0.159(1)	−0.503(1)	0.10(1)
C(13)	−0.122(2)	0.074(1)	−0.441(1)	0.08(1)
C(14)	−0.588(3)	−0.041(1)	−0.172(1)	0.12(2)
C(15)	−0.775(2)	−0.164(1)	−0.479(1)	0.09(1)
H(1)	−0.639 3	0.041 5	−0.417 2	0.058
H(21)	−0.394 4	0.024 7	−0.301 0	0.058
H(22)	−0.416 5	0.145 5	−0.351 9	0.058
H(31)	−0.648 6	0.131 6	−0.248 0	0.058
H(32)	−0.777 6	0.095 8	−0.317 8	0.058
H(5)	−0.814 7	−0.074 1	−0.337 2	0.058
H(61)	−0.600 4	−0.227 2	−0.251 3	0.058
H(62)	−0.460 0	−0.153 3	−0.286 4	0.058
H(71)	−0.501 7	−0.285 2	−0.374 9	0.058
H(72)	−0.749 2	−0.274 0	−0.355 0	0.058
H(9)	−0.329 3	−0.122 7	−0.398 8	0.058
H(101)	−0.533 0	−0.024 6	−0.525 1	0.058
H(102)	−0.237 1	−0.050 9	−0.517 3	0.058
H(121)	−0.317 0	0.187 3	−0.544 4	0.058
H(122)	−0.552 5	0.144 2	−0.526 4	0.058
H(123)	−0.430 0	0.218 2	−0.464 3	0.058
H(131)	−0.021 4	0.105 6	−0.480 6	0.058
H(132)	−0.111 7	0.128 0	−0.394 7	0.058

Table 5 (*continued*)

Caryophyllene nitrosite

	x/a	*y/b*	*z/c*	*U*
H(133)	−0.061 5	0.004 2	−0.422 8	0.058
H(141)	−0.617 7	−0.101 7	−0.137 0	0.058
H(142)	−0.581 9	0.025 8	−0.135 1	0.058
H(143)	−0.411 8	−0.054 9	−0.186 0	0.058
H(151)	−0.785 9	−0.107 4	−0.514 6	0.058
H(152)	−0.886 9	−0.227 3	−0.466 2	0.058

Dinitrocaryophyllene

	x/a	*y/b*	*z/c*	*U*
O(1)	0.675 1(4)	0.255 8(4)	0.096 8(3)	0.083(2)
O(2)	0.504 8(6)	0.256 4(4)	0.277 8(3)	0.102(3)
O(3)	0.729 3(4)	0.468 3(4)	−0.059 4(4)	0.098(3)
O(4)	0.587 8(6)	0.490 7(4)	0.131 1(4)	0.104(3)
N(1)	0.521 6(5)	0.275 2(3)	0.159 0(3)	0.065(2)
N(2)	0.592 1(5)	0.454 1(4)	0.018 7(4)	0.070(2)
C(1)	0.132 8(5)	0.242 4	−0.255 0(3)	0.048(2)
C(2)	0.064 5(6)	0.227 6(4)	−0.108 8(3)	0.058(2)
C(3)	0.237 1(8)	0.219 9(4)	0.005 0(4)	0.061(3)
C(4)	0.327 1(5)	0.317 7(4)	0.074 0(3)	0.052(2)
C(5)	0.407 1(5)	0.390 7(4)	−0.034 2(3)	0.050(2)
C(6)	0.241 6(6)	0.467 2(4)	−0.090 3(4)	0.057(2)
C(7)	0.280 9(7)	0.506 3(4)	−0.233 3(4)	0.066(2)
C(8)	0.282 7(5)	0.421 5(4)	−0.337 2(3)	0.058(2)
C(9)	0.106 4(6)	0.345 8(4)	−0.336 6(3)	0.056(2)
C(10)	0.051 6(8)	0.279 4(5)	−0.463 9(4)	0.073(3)
C(11)	0.004 1(6)	0.187 2(4)	−0.373 4(3)	0.061(2)
C(12)	−0.227 8(7)	0.180 0(6)	−0.349 6(6)	0.083(4)
C(13)	0.086 7(10)	0.083 1(5)	−0.412 5(6)	0.086(4)
C(14)	0.178 9(7)	0.365 5(5)	0.170 4(4)	0.072(3)
C(15)	0.434 8(7)	0.416 2(5)	−0.422 3(4)	0.078(3)
H(1)	0.281(5)	0.221(3)	−0.263(3)	0.040(8)
H(5)	0.462(4)	0.349(2)	−0.101(3)	0.039(7)
H(9)	−0.008(7)	0.378(4)	−0.311(4)	0.08(1)
H(21)	−0.003(6)	0.164(3)	−0.107(4)	0.07(1)
H(22)	−0.043(7)	0.278(4)	−0.091(4)	0.08(1)
H(31)	0.204(5)	0.173(3)	0.079(4)	0.065(8)
H(32)	0.343(7)	0.185(5)	−0.028(5)	0.05(2)
H(61)	0.242(5)	0.522(3)	−0.025(4)	0.064(9)
H(62)	0.103(6)	0.434(3)	−0.098(3)	0.058(9)
H(71)	0.391(7)	0.544(4)	−0.232(4)	0.07(1)
H(72)	0.184(6)	0.554(3)	−0.256(4)	0.071(9)
H(101)	−0.040(9)	0.298(4)	−0.525(6)	0.09(1)
H(102)	0.180(8)	0.264(4)	−0.512(4)	0.08(1)
H(121)	−0.302(7)	0.155(3)	−0.432(4)	0.08(1)
H(122)	−0.288(8)	0.242(5)	−0.317(5)	0.08(2)
H(123)	−0.260(9)	0.137(5)	−0.269(6)	0.09(2)
H(131)	0.036(9)	0.056(5)	−0.487(6)	0.09(1)
H(132)	0.066(9)	0.033(6)	−0.332(6)	0.11(2)
H(133)	0.210(10)	0.096(5)	−0.446(6)	0.10(2)
H(141)	0.157(7)	0.313(4)	0.229(5)	0.08(1)
H(142)	0.234(8)	0.412(4)	0.224(5)	0.08(1)
H(143)	0.057(6)	0.390(3)	0.116(4)	0.049(9)
H(151)	0.433(8)	0.355(5)	−0.493(6)	0.10(2)
H(152)	0.547(7)	0.470(4)	−0.413(4)	0.08(1)

(iiia) The E.p.r. Spectra of the Radical that is Obtained on Red-irradiating a Solid Solution of Caryophyllene Nitrosite in Dinitrocaryophyllene.—Earlier polycrystalline e.p.r. work shows that several nitroxide radicals can be obtained from caryophyllene nitrosite, and that in some of them the unpaired electron is coupled to more than one magnetic nucleus.[23,27] In these circumstances it is notoriously difficult to obtain exact, and even unambiguous, spin-Hamiltonian parameters from polycrystalline e.p.r. spectra, for the principal axes of the various tensors do not then always coincide: furthermore, information about the orientations of radicals cannot be obtained from

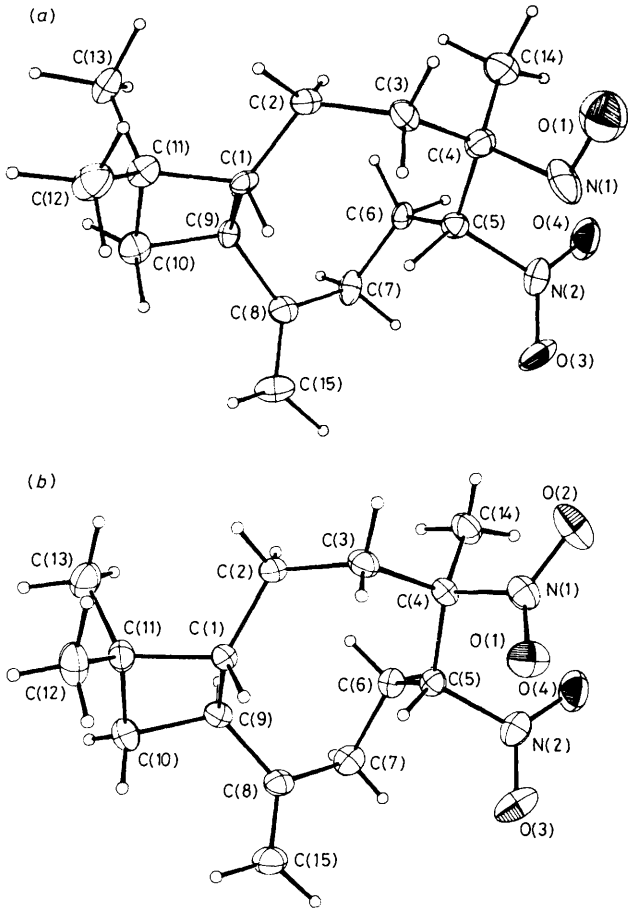

Figure 1. Molecular conformations in caryophyllene nitrosite, (*a*), and dinitrocaryophyllene, (*b*)

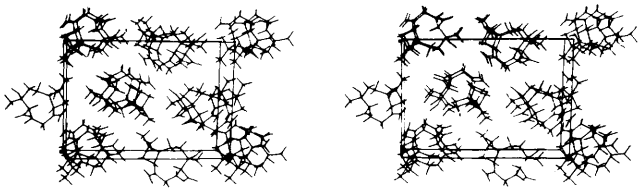

Figure 2. Stereoscopic view of the molecular packing within the unit cell of caryophyllene nitrosite

polycrystalline analysis. Precise and detailed information about the magnetic properties of these radicals, and their orientations in the unit cell, is important in understanding the mechanisms of the photochemical reactions in the solid, and we therefore examined single-crystal e.p.r. spectra after irradiating caryophyllene nitrosite with red light. Attempts to grow single crystals of pure caryophyllene nitrosite were unsuccessful, long needles unsuitable for e.p.r. purposes were always obtained, but good single crystals of dinitrocaryophyllene doped with 10% of caryophyllene nitrosite were grown from ethanol, and these were used: the *X*-ray diffraction pattern of the mixed crystal is almost the same as that obtained from pure dinitrocaryophyllene.

After identifying the right-handed orthogonal co-ordinate framework, *xyz*, shown in Figure 4, the crystal was mounted along its $+y$ axis inside a standard $T.E._{102}$ rectangular cavity of a Decca e.p.r. spectrometer, and then equally irradiated on all sides with red light. When a suitable concentration of radicals was obtained, e.p.r. spectra were recorded with the magnetic

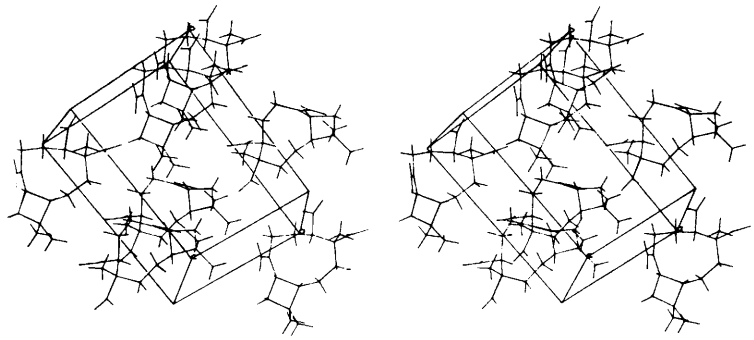

Figure 3. Stereoscopic view of the molecular packing within the unit cell of dinitrocaryophyllene

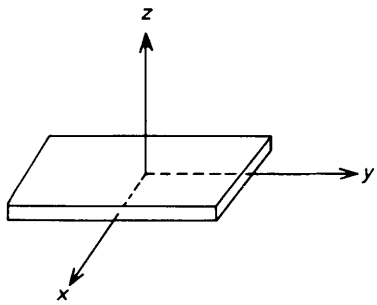

Figure 4. Right-handed orthogonal framework

field along the $+z$ direction, and then, with the field still in the zx plane, at angles, θ, of 15°, 30° ... to the $+z$ direction. The same crystal was then remounted (*i*), along the $+z$ and (*ii*), along the $+x$ directions and the experiment repeated with the magnetic field in the xy and yz planes, respectively. Some of the single-crystal spectra are shown in Figure 5. Finally, *X*-ray rotation and Weissenberg photographs of the same crystal were taken in order to relate the xyz frame with the frame of the crystallographic unit cell, *abc*: the *X*-ray photographs showed no evidence of phase separation on irradiating this mixed crystal. The transformation relations connecting the two frames turned out to be.

$$\begin{pmatrix} x \\ y \\ z \end{pmatrix} = \begin{pmatrix} 0 & 1 & 0 \\ 1 & 0 & 0 \\ 0 & 0 & -\sin\beta \end{pmatrix} \begin{pmatrix} a \\ b \\ c \end{pmatrix}$$

E.p.r. spectra recorded with the magnetic field in the yz plane, *i.e.*, the *ac* plane of the unit cell, consist of six peaks, and are characteristic of a nitroxide radical in which one unpaired electron interacts with one ^{14}N nucleus and with one proton. Its spin-Hamiltonian was assumed to have the form of equation (1),

$$\mathcal{H} = \beta_e H.g.S + S.A(^{14}N).I(^{14}N) + S.A(^{1}H).I(^{1}H) \quad (1)$$

and g, $A(^{14}N)$, and $A(^{1}H)$ tensor components for each orientation in this plane were easily extracted from these spectra. The squares of these parameters were least-squares fitted to curves of the form of equation (2), where W is a

$$W^2 = W_{yy}\cos^2\theta + 2W_{yz}\cos\theta\sin\theta + W_{zz}\sin^2\theta \quad (2)$$

measured g, or $A(^{14}N)$ or $A(^{1}H)$ component, and the components W_{yy}, W_{yz}, and W_{zz}, respectively, of the squares of the g, $A(^{14}N)$, and $A(^{1}H)$ tensors thus obtained. Except for

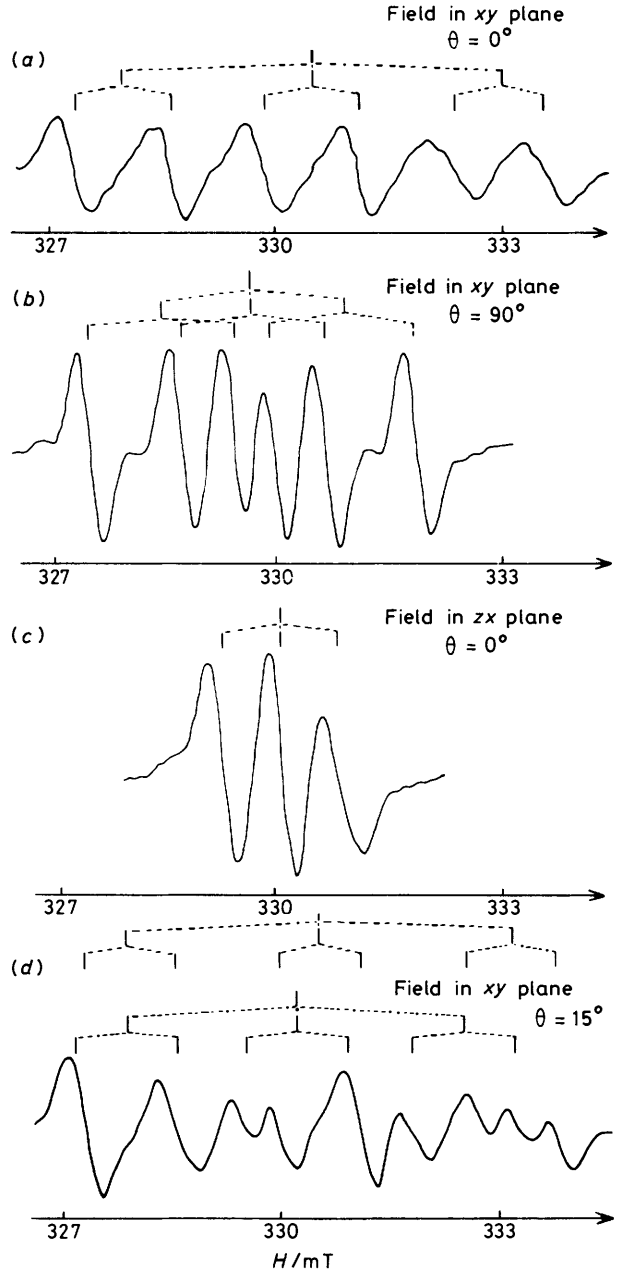

Figure 5. E.p.r. spectra of the radical (**11**) that is obtained by red-irradiating a single crystal of caryophyllene nitrosite in dinitrocaryophyllene (1:9). The magnetic field is directed along the x axis in (*a*), along the y axis in (*b*), along the z axis in (*c*), and in the xy plane at 15° to the x axis in (*d*)

Table 6. Components of the squares of the g, $A(^{14}N)$ and $A(^{1}H)$ tensors referred to the xyz frame, for the two chemically equivalent but crystallographically distinguishable radicals (**11**) obtained when caryophyllene nitrosite doped into dinitrocaryophyllene (1:9) is irradiated with red light. Hyperfine tensor components are in mT^2. For reasons explained in the text, two sets of data are consistent with the e.p.r. results

	Radical (**11**), site A	Radical (**11**), site B
g^2	$\begin{pmatrix} 4.014\,99 & 0.005\,16 & 0.000\,1 \\ 0.005\,16 & 4.034\,52 & -0.003\,56 \\ 0.000\,1 & -0.003\,56 & 4.027\,41 \end{pmatrix}$	$\begin{pmatrix} 4.014\,99 & -0.005\,16 & -0.000\,1 \\ -0.005\,16 & 4.034\,52 & -0.003\,56 \\ -0.000\,1 & -0.003\,56 & 4.027\,41 \end{pmatrix}$
$[A(^{14}N)]^2$	$\begin{pmatrix} 7.524 & -2.055 & 0.403 \\ -2.055 & 1.654 & -0.387 \\ 0.403 & -0.387 & 0.377 \end{pmatrix}$	$\begin{pmatrix} 7.524 & 2.055 & -0.403 \\ 2.055 & 1.654 & -0.387 \\ -0.403 & -0.387 & 0.377 \end{pmatrix}$
$[A(^{1}H)]^2$	$\begin{pmatrix} 1.575 & 0.445 & 0.055 \\ 0.445 & 3.935 & 0.483 \\ 0.055 & 0.483 & 0.065 \end{pmatrix}$	$\begin{pmatrix} 1.575 & -0.445 & -0.055 \\ -0.445 & 3.935 & 0.483 \\ -0.055 & 0.483 & 0.065 \end{pmatrix}$
OR		
	Radical (**11**), site A′	Radical (**11**), site B′
g^2	$\begin{pmatrix} 4.014\,99 & 0.005\,16 & -0.000\,1 \\ 0.005\,16 & 4.034\,52 & -0.003\,56 \\ -0.000\,1 & -0.003\,56 & 4.027\,41 \end{pmatrix}$	$\begin{pmatrix} 4.014\,99 & -0.005\,16 & 0.000\,1 \\ -0.005\,16 & 4.034\,52 & -0.003\,56 \\ 0.000\,1 & -0.003\,56 & 4.027\,41 \end{pmatrix}$
$[A(^{14}N)]^2$	$\begin{pmatrix} 7.524 & -2.055 & -0.403 \\ -2.055 & 1.654 & -0.387 \\ -0.403 & -0.387 & 0.377 \end{pmatrix}$	$\begin{pmatrix} 7.524 & 2.055 & 0.403 \\ 2.055 & 1.654 & -0.387 \\ 0.403 & -0.387 & 0.377 \end{pmatrix}$
$[A(^{1}H)]^2$	$\begin{pmatrix} 1.575 & 0.445 & -0.055 \\ 0.445 & 3.935 & 0.483 \\ -0.055 & 0.483 & 0.065 \end{pmatrix}$	$\begin{pmatrix} 1.575 & -0.445 & 0.055 \\ -0.445 & 3.935 & 0.483 \\ 0.055 & 0.483 & 0.065 \end{pmatrix}$

special directions, spectra recorded with the magnetic field in the zx or xy planes are more complex, since in general they arise from overlapping of six-peaked spectra of two chemically identical but crystallographically distinguishable nitroxide radicals, but these were unravelled when it was realized that in these two planes the spectrum of one radical recorded at an orientation θ is the same as that of the second radical recorded at an orientation $(180° - \theta)$: these geometrical relationships are those expected for the monoclinic space group $P2_1$ when the unit cell contains two molecules related to each other by the two-fold screw axis. The squares of the g, $A(^{14}N)$, and $A(^{1}H)$ tensors for the two crystallographically distinguishable radicals are given in Table 6. Two sets of data fit the e.p.r. results because of the ambiguity in matching up relative signs of the xy and zx off-diagonal elements of the tensors of the two crystallographically different radicals. Though they are small, these off-diagonal elements are real. We were unable to discriminate between the two sets of tensors by examining spectra at other intermediate orientations and, in fact, calculations show that at the orientation for which the differences in the magnetic properties of the several sets of data are maximized, the differences would not be significantly greater than the experimental uncertainties in the measurements.

When diagonalized, the data in Table 6 yield the principal values of the various tensors in the spin-Hamiltonian, and their corresponding direction cosines with respect to the xyz frame, that are listed in Table 7.

The data in Table 7 confirm that the two radicals are nitroxide radicals, that they are chemically equivalent although crystallographically, and therefore magnetically, distinguishable, that the principal directions of the second of these radicals are obtained by rotating the principal axes of the first radical through 180° about the x axis, and that the principal directions of the g, $A(^{14}N)$, and $A(^{1}H)$ tensors do not coincide, although the $A(^{14}N)$ frame is rotated by only a few degrees from that of g. Furthermore, the magnitudes of the principal values of the proton hyperfine coupling tensor identify it as an α-proton and therefore these radicals are monoalkyl nitroxide radicals R–HN$\dot{-}$O. The signs of each of the three principal values of $A(^{1}H)$ are therefore negative and the corresponding principal values of $A(^{14}N)$ are all positive.

In nitroxide radicals the largest principal component of the g tensor is obtained when the applied magnetic field is nearly parallel to the N–O bond, and the smallest principal component of (g), and the largest principal component of the ^{14}N hyperfine coupling tensor is obtained when the field lies nearly parallel to the axis of the p_z orbital of the nitrogen atom.[28–30] The proton hyperfine coupling tensor $[A(^{1}H)]$ can be decomposed into its Fermi contact and direct dipolar components to give:

$$A(^{1}H)\ (mT) = \begin{pmatrix} -1.105 & & \\ & -1.105 & \\ & & -1.105 \end{pmatrix} + \begin{pmatrix} -0.117 & & \\ & -0.914 & \\ & & +1.030 \end{pmatrix}$$

where the direction cosines of the principal anisotropic components are listed in Table 7. Examination of the $A(^{1}H)$ principal axes directions shows, as is expected, that the −0.117 mT anisotropic component lies almost parallel to the axis of the $2p_z$ orbital on the nitrogen atom. The +1.030 mT principal component lies almost parallel to the N–H bond direction, and the −0.914 mT component lies close to the σ-framework of the nitroxide radical, at 90° to the N–H bond direction. The orientations of the principal directions of the g and $A(^{1}H)$ tensors in the molecular frame are shown in Figure 6. The data in Table 7 enable the two crystallographically distinguishable radicals to be orientated in the crystal framework and the results are shown in Figure 7. The σ-frameworks of the radicals lie approximately in the yz plane of the crystal, the ac^* plane of the unit cell, and the axis of the $2p_z$ orbital of the nitrogen atom lies close to the x direction of the crystal, the b axis direction of the unit cell.

The conformations of the parent molecules and their orientations in the crystal, the proximity of the C(5)–H hydrogen atom to the nitroso group, the structures of the

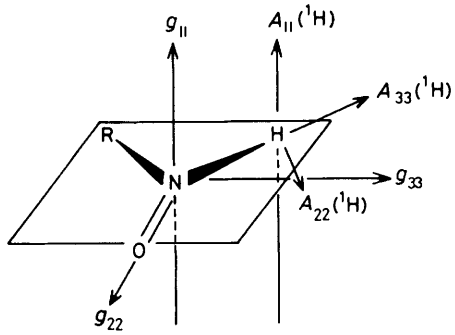

Figure 6. The principal directions of the g and $A(^1H)$ tensors orientated in the R–HN=O frame of radical (**11**)

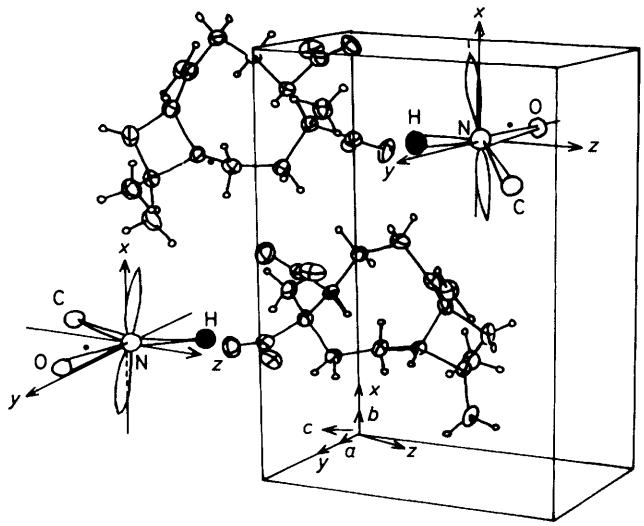

Figure 7. The orientations of the two crystallographically distinguishable nitroxide radicals (**11**) in the host dinitrocaryophyllene unit cell

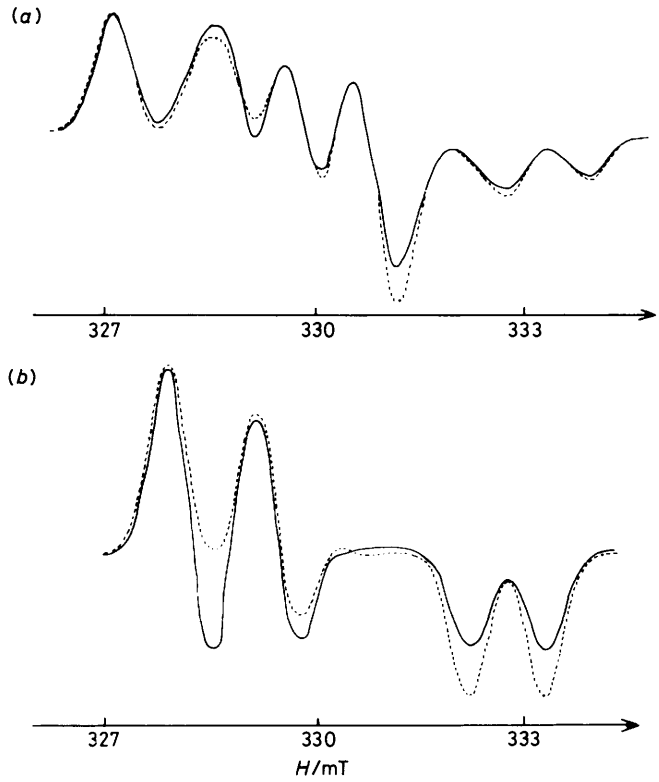

Figure 8. E.p.r. spectra of radicals (**11**) obtained by irradiating a polycrystalline solid solution of caryophyllene nitrosite in dinitrocaryophyllene (1:9) with red light. (*a*) is obtained from the naturally occurring nitrogen isotopic mixture, and (*b*) is obtained from ^{15}N-labelled caryophyllene nitrosite in normal ^{14}N-dinitrocaryophyllene (1:9). The dotted line in (*a*) is the spectrum calculated using the spin-Hamiltonian parameters in Table 7. The dotted line in (*b*) is calculated using these same parameters but with the $A(^{14}N)$ values scaled by the ratio $[\gamma(^{15}N)/\gamma(^{14}N)] = -1.402\,4$

radicals, and their orientations in the host dinitrocaryophyllene unit cell all show that on red-irradiating caryophyllene nitrosite in this host lattice, the $\pi^* \longleftarrow n$ excitation is followed by transfer of the C(5)–H hydrogen atom, and the intermediate biradical is then stabilized by loss of a hydrogen atom at C(6) to form the nitroxide radical (**11**), the species observed in the e.p.r. experiment.

Figure 8(*a*) shows the e.p.r. spectrum that is obtained when a polycrystalline solid solution of caryophyllene nitrosite in dinitrocaryophyllene (1:9) is irradiated with red light. The form of this spectrum does not change during the irradiation process, but its intensity rises to a maximum after about 12 h irradiation with our light source, and then decreases until, after about 50 h irradiation, all the blue coloration disappears and only a weak residual spectrum remains. When the irradiated crystals are kept in darkness the radical concentration starts to decay after about ten days. Figure 8(*b*) is a corresponding e.p.r. spectrum obtained from a red-irradiated solid solution of ^{15}N-labelled caryophyllene nitrosite in normal ^{14}N-dinitrocaryophyllene (1:9). It shows quite clearly that the nitroxide nitrogen nucleus in this radical is now exclusively ^{15}N-labelled, *i.e.*, the nitroxide nitrogen is derived exclusively from the original nitroso group of the red-irradiated caryophyllene nitrosite in these crystals.

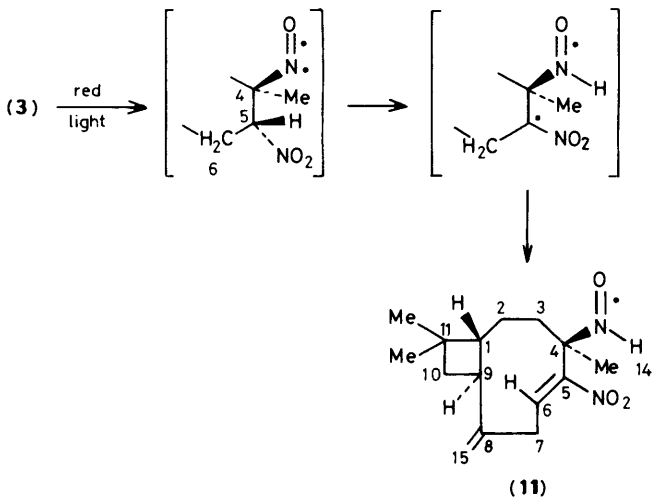

(**11**)

When the red-irradiated polycrystalline solution of caryophyllene nitrosite in dinitrocaryophyllene is dissolved in chloroform, another, different, nitroxide radical is formed. In this, the unpaired electron again interacts with one ^{14}N nucleus and with one proton, but its isotropic spin-Hamiltonian parameters are $\langle g \rangle = 2.006\,7(2)$, $a(^{14}N) = 1.40(3)$ mT, and $a(^1H) = 0.30(3)$ mT, parameters that are characteristic of a radical whose structure is (**12**). Monoalkyl nitroxide radicals disproportionate in liquid solution to form the corresponding nitrosoalkane and hydroxylamine, and compound (**11**) must form (**13**) and (**14**).

The nitroxide radical (**12**) may be formed by addition of an aliphatic nitrosoalkane to the endocyclic *trans* olefinic residue

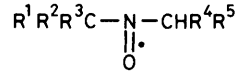

(12)

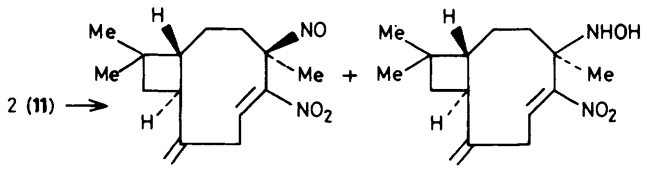

(13) (14)

of compound (**13**). The nitrosoalkane could be caryophyllene nitrosite, or even another molecule of compound (**13**). The reaction could involve either an 'ene' mechanism[31] similar to that described by Motherwell and Roberts,[27] or a one-electron-transfer mechanism similar to that described by Mulvey and Waters.[32]

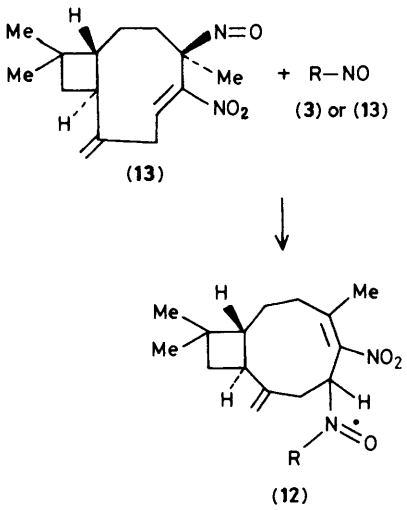

(13) (12)

(iiib) Polycrystalline E.p.r. Studies of the Radicals that are formed when Caryophyllene Nitrosite is Irradiated with Red Light.—Figure 9 shows e.p.r. spectra obtained at different times when a polycrystalline sample of caryophyllene nitrosite is irradiated with red light. The nature and the relative amounts of the radicals that are produced vary with irradiation time, and with our light source the production of radicals is stabilized after *ca.* 90 h. Figure 9E is the spectrum of the viscous yellow liquid that is finally obtained on complete irradiation.

The e.p.r. spectrum of this same viscous liquid dissolved in chloroform is shown in Figure 10. If this solution, in its turn, is then allowed to stand for some time, then a simple 1 : 1 : 1 triplet, characteristic of a ditertiaryalkyl nitroxide radical (**15**) is finally obtained. Figure 10 can be synthesized by superimposing e.p.r. spectra of radical (**15**) and radical (**12**). The e.p.r. spectrum obtained from solid material enriched in radical (**15**) is shown in

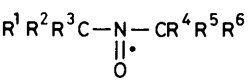

(15)

Figure 11, and if the spin-Hamiltonian parameters are written in the form $\mathscr{H} = \beta_e\, H.g.S + S.A(^{14}N).I(^{14}N)$, then this figure

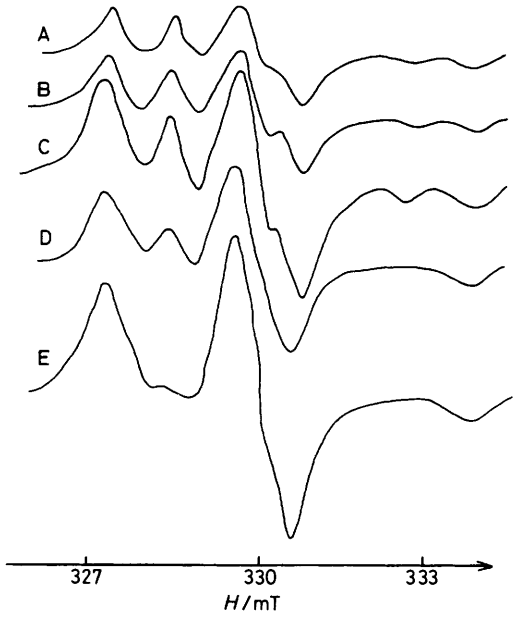

Figure 9. E.p.r. spectra of a polycrystalline sample of caryophyllene nitrosite irradiated, at 290 K, with red light: A, 2; B, 6; C, 14; D, 36; and E, 90 h

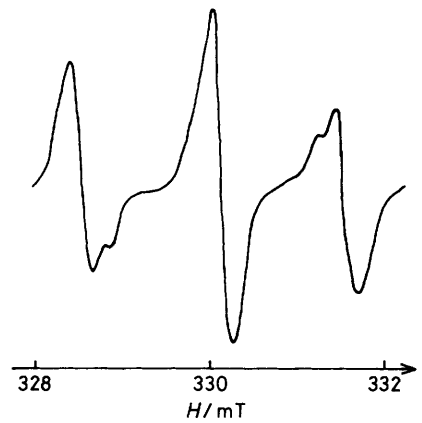

Figure 10. E.p.r. spectrum, at 290 K, of a dilute ethanol-free $CHCl_3$ solution of the viscous yellow liquid, Figure 9E, obtained by irradiating solid carophyllene nitrosite with red light

can be analysed in terms of a superposition of three curves of the type described by Kneubuhl[33] and the apparent principal components of the *g*-and $A(^{14}N)$-tensors, along with the line-broadening parameter, β, can be obtained from it. The parameters thus obtained are $g_{11} = 2.001\,9(3)$; $g_{22} = 2.006\,5(3)$; $g_{33} = 2.008\,9(3)$; $A_{11}(^{14}N) = 3.40(5)$ mT; $A_{22}(^{14}N) = 0.45(5)$ mT; $A_{33}(^{14}N) = 0.80(5)$ mT; $\beta = 0.25(5)$ mT.

Figure 9A—C shows that radicals (**15**) and (**12**) are not the primary paramagnetic species produced in the early stages of the solid-state photochemical reaction. Difference spectra obtained by subtracting a suitably scaled version of the spectrum in Figure 11 from the spectra in Figure 9 are almost identical with the spectrum in Figure 8(*a*), and they show that in the early stages the major nitroxide radical has structure (**11**), and that the concentration of (**11**) rises to a maximum and then decays on further irradiation with red light.

(iv) The Solid-state Photolysis Reaction Mechanisms.—All the information obtained from the chemical, *X*-ray, and e.p.r. studies

Table 7. Principal values and direction cosines of the g, $A(^{14}N)$, and $A(^{1}H)$ tensors, referred to the xyz frame, for the two chemically equivalent but crystallographically distinguishable radicals (**11**) obtained when caryophyllene nitrosite doped into dinitrocaryophyllene (1 : 9) is irradiated with red light. The direction cosine matrices are in the form

$$\begin{pmatrix} l_1 & l_2 & l_3 \\ m_1 & m_2 & m_3 \\ n_1 & n_2 & n_3 \end{pmatrix}$$

where l_1, m_1, n_1 are the directional cosines of principal component 1 with respect to the x, y, and z axes, (*i.e.*, with respect to the b, a, and c^* axes of the unit cell), ... *etc.* Hyperfine coupling components are in mT

	Radical (**11**), site A		Radical (**11**), site B	
g	2.003 40(5)		2.003 40(5)	
		2.009 2(1)		2.009 2(1)
		2.006 54(5)		2.006 54(5)
	0.965 4 −0.213 2 −0.150 5		0.965 4 −0.213 2 −0.150 5	
	−0.250 8 −0.917 0 −0.310 2		0.250 8 0.917 0 0.310 2	
	−0.071 9 0.337 2 −0.938 7		0.071 9 −0.337 2 0.938 7	
$[A(^{14}N)]$	2.864(13)		2.864(13)	
		1.044(2)		1.044(2)
		0.513(6)		0.513(6)
	0.951 1 −0.306 6 −0.037 6		0.951 1 −0.306 6 −0.037 6	
	−0.302 2 −0.898 5 −0.318 5		0.302 2 0.898 5 0.318 5	
	0.063 9 0.314 3 −0.947 2		−0.063 9 −0.314 3 0.974 2	
$[A(^{1}H)]$	−1.222(7)		−1.222(7)	
		−2.020(17)		−2.020(17)
		−0.075(100)		−0.075(100)
	0.984 1 −0.177 8 0.000 0		0.984 1 −0.177 8 0.000 0	
	−0.176 5 −0.976 7 0.122 1		0.176 5 0.976 7 −0.122 1	
	−0.021 8 −0.120 1 −0.992 5		0.021 8 0.120 1 0.992 5	
OR				
	Radical (**11**), site A′		Radical (**11**), site B′	
g	2.003 40(5)		2.003 40(5)	
		2.009 2(1)		2.009 2(1)
		2.006 54(5)		2.006 54(5)
	0.966 8 −0.215 7 −0.137 3		0.966 8 −0.215 7 −0.137 3	
	−0.249 0 −0.915 4 −0.316 3		0.249 0 0.915 4 0.316 3	
	−0.057 5 0.340 0 −0.938 7		0.057 5 −0.340 0 0.938 7	
$A(^{14}N)$	2.86(1)		2.86(1)	
		1.128(5)		1.128(5)
		0.32(7)		0.32(7)
	0.953 9 −0.247 1 −0.170 6		0.953 9 −0.247 1 −0.170 6	
	−0.298 3 −0.844 4 −0.444 9		0.298 3 0.844 4 0.444 9	
	−0.034 1 0.475 3 −0.879 1		0.034 1 −0.475 3 0.879 1	
$A(^{1}H)$	−1.227(7)		−1.227(7)	
		−2.02(2)		−2.02(2)
		0.00(4)		0.00(4)
	0.982 3 −0.173 2 0.071 3		0.982 3 −0.173 2 0.071 3	
	−0.163 1 −0.978 1 0.129 5		0.163 1 0.978 1 −0.129 5	
	−0.092 2 −0.115 6 −0.989 0		0.092 2 0.115 6 0.989 0	

can now be pieced together and the sequence of photochemical reactions that take place when solid caryophyllene nitrosite is irradiated with red light thence unravelled. The reactions are summarized in the following Schemes A—E.

Absorption of red light causes the nitroso group to undergo an $\pi^* \longleftarrow$ n transition which then triggers off two main reaction pathways. In the first of these the nearby hydrogen atom on C(5) migrates to form the monoalkyl nitroxide radical (**11**). The second path arises because the $\pi^* \longleftarrow$ n transition not only weakens the N=O bond, it also weakens the C(4)–N bond, which then breaks to produce a master radical (**16**) and an excited nitric oxide molecule. This master radical is all-important in understanding the mechanisms involved in the further stages of the photolysis reaction. It is formed, not only in the primary reaction A, but also in a series of secondary reactions B, in which caryophyllene nitrosite reacts with two molecules of nitric oxide to form (**16**) plus NO_3· radicals and nitrogen. The NO* can be oxidized to NO_2. NO_2 can also be

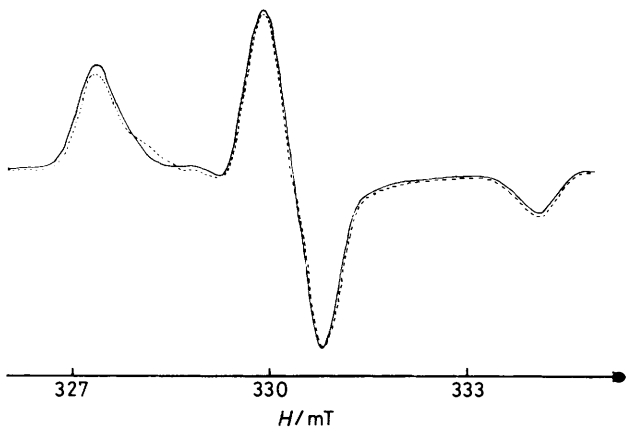

Figure 11. E.p.r. spectrum of a polycrystalline sample of solid material enriched in radical (**15**). The dotted line is the spectrum calculated using the spin-Hamiltonian parameters given in the text

produced by decomposition of the NO_3· radical formed in Scheme B. The master radical (**16**) then takes part in several different reactions as summarized in Schemes C—E.

In Scheme C, (**16**) is stabilized either by loss of NO_2 to give isocaryophyllene (**6**), or by loss of a hydrogen atom to form the olefins (**8**), (**9**), or (**10**). In Scheme D, the master radical (**16**) reacts with NO_2 to give dinitrocaryophyllene (**5**) or with NO_3· to give nitronitratocaryophyllene (**7**).

In Scheme E, the radical (**16**), produced by irradiating a molecule at the point (*x*,*y*,*z*) in the orthorhombic unit cell of caryophyllene nitrosite, is scavenged by a neighbouring nitrosite molecule displaced by the unit cell translation $-a$ from it, *i.e.*, scavenging of (**16**) by the parent molecule at the point [(*x* − *a*), *y*, *z*] produces the stable ditertiaryalkyl nitroxide radical (**15**). The crystal structure of caryophyllene nitrosite requires the configurations at the asymmetric centres and the conformation of the radical (**15**) to be as shown in Scheme E. Scheme E requires 'parallel' molecules, and these are available in the crystal structures of both (**3**) and (**5**). However, in the mixed crystal each caryophyllene nitrosite molecule is surrounded by dinitrocaryophyllene neighbours, and so the second reaction in Scheme E, and thence the formation of the ditertiaryalkyl nitroxide (**15**), is not observed in that case.

Radical (**11**), formed in Scheme A, undergoes further reaction to produce still another nitroxide radical whose structure is uncertain: it could be compound (**12**) and be a product of further reaction of compounds (**13**) or (**14**), disproportionation products of radical (**11**).

Experimental

Caryophyllene.—Technical grade caryophyllene (100 g) was dissolved in light petroleum (b.p. 40—60 °C; 100 ml) and thoroughly washed with sodium hydroxide (2M; 3 × 100 ml) followed by repeated washing with distilled water until the aqueous layer was neutral. The organic layer was then washed with aqueous silver nitrate solution (50%; 3 × 75 ml) to remove humulene. After washing with distilled water (3 × 100 ml), the petroleum extract was dried and the solvent removed to afford a colourless oil, which on fractional distillation gave pure caryophyllene, b.p. 118 °C at 9 mmHg.

Reaction of Caryophyllene with Oxides of Nitrogen.—A solution of caryophyllene (3 g) in light petroleum (7.5 ml) was cooled to 10 °C. Saturated aqueous $NaNO_2$ (2 g) was also cooled to 10 °C and the two solutions were then mixed. Glacial acetic acid (1.2 ml) was then added dropwise with continual stirring during 15 min. The light petroleum layer turned blue-green, and when left for 30 min at 0 °C an oily blue solid precipitated out. This solid was filtered off and washed with light petroleum to remove the oil, which was characterized (^{1}H n.m.r.) as unchanged caryophyllene. This caryophyllene was treated with an excess of N_2O_3 to obtain more blue crystals. Each cycle produced a crude product that became greener and eventually a yellow oil was the sole reaction product. Recrystallization of the blue solid from ethanol yielded blue needles. T.l.c. on silica [ether–light petroleum (1 : 1 v/v) as eluant] showed the presence of two components of R_F 0.59 and 0.64. A sample (400 mg) was chromatographed on silica [1.5 m column; ether–light petroleum (1 : 1 v/v) as eluant] and twelve 10-ml fractions were collected.

Fractions 1—6, R_F 0.64, contained caryophyllene nitrosite (4,11,11-trimethyl-8-methylene-5-nitro-4-nitrosobicyclo[7.2.0]-undecane) (**3**) (Found: C, 64.4; H, 8.4; N, 10.3; O, 16.9. $C_{15}H_{24}N_2O_3$ requires C, 64.3; H, 8.6; N, 10.0; O, 17.15%); m.p. 116—117 °C; δ_H ($CDCl_3$) 5.92 (1 H, m, 5-H), 5.25 (2 H, br s, 15-H_2), 2—2.6 (5 H, m, 9-H, 7-H_2, 1-H, and one of 6-H_2), 1.4—2 (7 H, m, 2-H_2, 3-H_2, one of 6-H_2, and 10-H_2), 1.18 (3 H, s, 14-H_3, 1.00 (6 H, s, 12-H_3 and 13-H_3); ^{13}C-{^{1}H} decoupled spectrum chemical shifts (p.p.m.) 59.23(d, C-1), 23.31(t, C-2), 36.92(t, C-3), 100.81(s, C-4), 88.01(d, C-5), 28.27(t, C-6), 35.11(t, C-7), 148.46(s, C-8), 42.65(d, C-9), 36.10(t, C-10), 38.89(s, C-11), 21.59(q, C-12), 29.59(q, C-13), 13.82(q, C-14), 113.22(t, C-15); $\nu_{max.}$ (KBr disc) 3 085 [=C(15)-H_2], 3 000, 2 960, 2 950, 2 930, and 2 870 (C-H), 1 646 and 905 [C(8)=C(15)], 1 578 (N=O), 1 554, 1 350, and 852 (RNO_2), 1 385 and 1 380 cm^{-1} (>CMe_2); *m*/*z* 250, 204, 203, 190, and 189 [the parent peak for $C_{15}H_{24}N_2O_3$, expected at 280, was not observed since the NO group is cleaved inside the mass spectrometer; the peak at 250 originates from an ion of the 'master' aliphatic radical (**16**)].

Fractions 7—12, R_F 0.59, contained dinitrocaryophyllene (4,11,11-trimethyl-8-methylene-4,5-dinitrobicyclo[7.2.0]un-decane) (**5**) (Found: C, 60.6; H, 7.9; N, 9.6; O, 21.9. $C_{15}H_{24}N_2O_4$ requires C, 60.9; H, 8.1; N, 9.5; O, 21.5%); m.p. 126—127 °C; δ_H ($CDCl_3$) 5.19 (2 H, br s, 15-H_2), 5.15 (1 H, t, X of ABX spectrum, J_{AX} + J_{BX} 16 Hz, 5-H), 2—2.7 (6 H, m, 9-H, 7-H_2, 1-H, one of 6-H_2, and one of 3-H_2) 1.5—2 (6 H, m, one of 3-H_2, one of 6-H_2, 2-H_2, and 10-H_2), 1.94 (3 H, s, 14-H_3), 1.00 and 1.02 (6 H, 2 × s, 12-H_3 and 13-H_3); ^{13}C-{^{1}H} decoupled spectrum 57.82(d, C-1), 23.85(t, C-2), 43.63(t, C-3), 92.60(s, C-4), 86.20(d, C-5), 29.98(t, C-6), 35.10(t, C-7), 147.81(s, C-8), 42.18(d, C-9), 36.04(t, C-10), 34.69(s, C-11), 21.66(q, C-12), 29.62(q, C-13), 18.06(q, C-14), 113.62(t, C-15); $\nu_{max.}$ (KBr disc) 3 080 [=C(15)-H_2], 2 960, 2 900, and 2 870 (C-H), 1 640, 1 630, and 910 [C(8)=C(15)-H_2], 1 560, 1 364, and 863 [C(4)-NO_2], 1 548, 1 345, and 850 cm^{-1} [C(5)-NO_2]; *m*/*z* 296, 280, 250, and 204.

Photolysis of Solid Caryophyllene Nitrosite with Red Light.—Pure solid caryophyllene nitrosite (1 g) was placed in a flask that was evacuated and sealed, and the nitrosite was then irradiated with red light, at 20 °C, until the blue crystals were completely converted into a yellow viscous oil. I.r. and ^{1}H n.m.r. examination of this oil revealed the disappearance of the nitroso group, retention of the exocyclic double bond and the nitro group of caryophyllene nitrosite, and formation of a nitrate, several olefinic species, and a small amount of a carbonyl-containing compound.

When the yellow oil is shaken with light petroleum (b.p. 40—60 °C) *ca.* 50% of it dissolves to give a clear solution which was then decanted and the light petroleum evaporated off to yield a clear oil. The insoluble fraction is a viscous yellow oil that is soluble in chloroform.

The total photolysis products and the fractions soluble and insoluble in light petroleum were separated by preparative t.l.c.

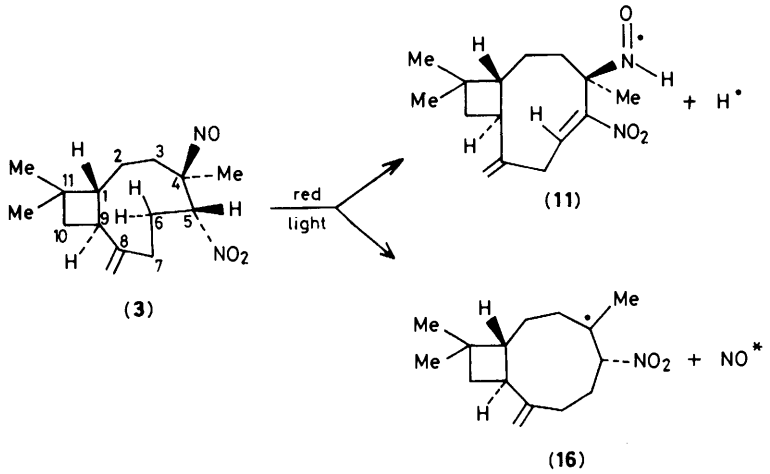

Scheme A

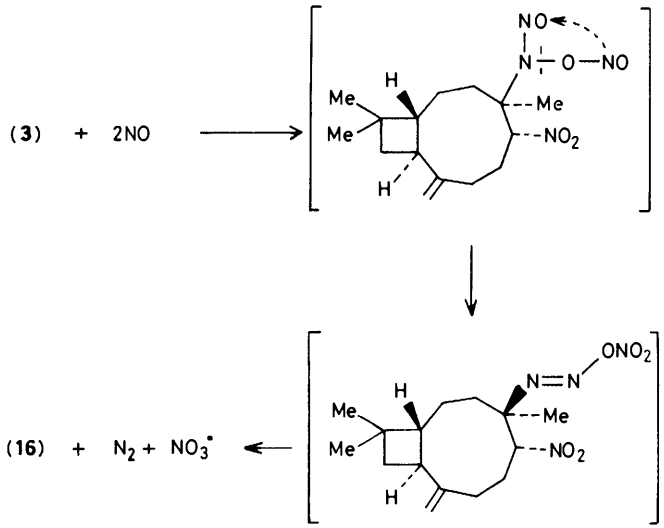

Scheme B

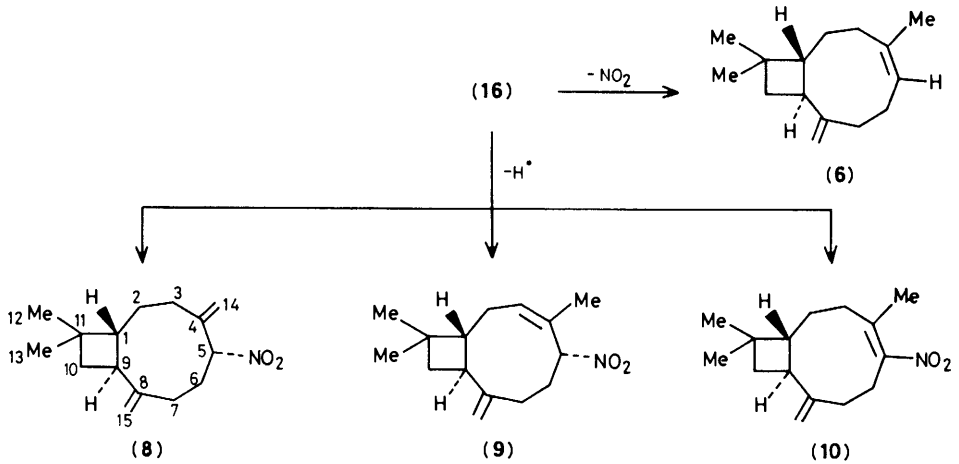

Scheme C

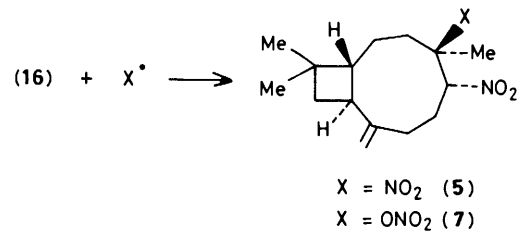

Scheme D

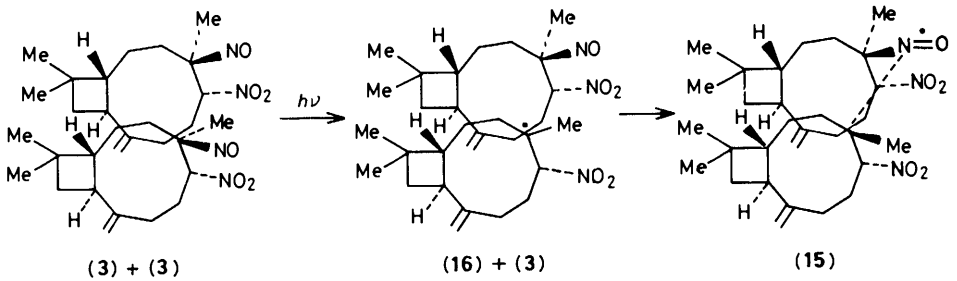

Scheme E

on silica plates using hexane–ethyl acetate (1:1 v/v) as eluant. T.l.c. reveals the presence of at least 14 components in the photolysis mixture.

The fraction insoluble in light petroleum contains at least nine components that can be separated into three groups. The first, $R_F = 0$, forms a viscous yellow-brown oil that is paramagnetic, yielding a magnetically dilute polycrystalline e.p.r. spectrum and a 1:1:1 triplet e.p.r. spectrum in $CHCl_3$ solution, spectra that are characteristic of a di-tertiary-alkyl nitroxide radical. The second, $0.05 \leqslant R_F \leqslant 0.2$, contains four components whose i.r. spectra reveal the loss of the exocyclic olefinic residue of the caryophyllene skeleton and a very strong intensity enhancement of the R-NO_2 region: ^{1}H n.m.r. spectra confirm the absence of olefinic residues. This second insoluble fraction seems to consist of polynitrated derivatives obtained by NO_2 addition to the exocyclic double bond of dinitrocaryophyllene. The third group, $0.2 \leqslant R_F \leqslant 0.35$, again contains four components whose i.r. spectra reveal the presence of exocyclic olefinic, R-ONO_2, and R-NO_2 residues.

Chromatographing the light petroleum-soluble fraction on 2 mm 20 × 20 cm silica plates using hexane–ethyl acetate (2.5:1) as eluant reveals the presence of four main products of R_F 0.41, 0.47, 0.55, and 0.67.

The component R_F 0.41, 10% of the total photolysis products, is a white crystalline solid, identified as dinitrocaryophyllene (**5**).

The component R_F 0.47, 10% of the total photolysis products, is a white crystalline solid that can be recrystallized from ethanol, m.p. 93—94 °C. ^{1}H, ^{13}C n.m.r., i.r., and mass spectra show that this component is nitronitratocaryophyllene (4,11,11-trimethyl-8-methylene-4-nitrato-5-nitrobicyclo[7.2.0]undecane), (**7**), δ_H ($CDCl_3$) 5.06 (1 H, t, 5-H), 5.10 and 5.02 (2 H, AB spectrum, J_{AB} 2 Hz, 15-H_2), 1.9—2.5 (7 H, m, 9-H, 7-H_2, 1-H, 6-H_2, and one of 3-H_2), 1.68 (3 H, s, 14-H_3), 1.1—1.9 (5 H, m, 2-H_2, one of 3-H_2, and 10-H_2), 0.99 and 1.02 (6 H, 2 × s, 12-H_3 and 13-H_3); ^{13}C-{^{1}H} decoupled spectrum 57.89(d, C-1), 23.92(t, C-2), 37.95(t, C-3), 91.97(s, C-4), 87.86(d, C-5), 28.25(t, C-6), 34.75(t, C-7), 148.05(s, C-8), 42.48(d, C-9), 35.94(s, C-10), 34.79(s, C-11), 21.59(q, C-12), 29.68(q, C-13), 18.32(q, C-14), 113.13(t, C-15); $\nu_{max.}$ (KBr disc) 3 080 [=C(15)-H_2], 2 965, 2 940, 2 900, and 2 860 (C-H), 1 634, and 910 [C(8)=C(15)-H_2], 1 625, 1 290, and 845 (R-ONO_2), 1 555, 1 370, and 850 (R-NO_2), 1 390 cm^{-1} (>CMe_2); *m/z* 266, 220, 205, 204, and 203 (the parent peak for $C_{15}H_{24}N_2O_5$, expected at 312, was not observed since the -O-NO_2 group is cleaved inside the mass spectrometer; the peak at 266 is $M^+ - NO_2$).

The component R_F 0.55, 10% of the total photolysis products, is a clear oil, and is a mixture of compounds that we have not managed to separate. I.r., ^{1}H, and ^{13}C n.m.r. spectra reveal an average of one NO_2 residue per molecule (including a small amount of conjugated NO_2), four different exomethylene residues, and two endocyclic double bonds. On the basis of ^{1}H, ^{13}C n.m.r., i.r., and mass spectra this component is shown to contain the nitro-olefin (**8**) and its isomers (**9**) and (**10**): δ_H ($CDCl_3$) 5.70 (<1 H, m), 5.37 (<1 H, d), 4.94 (*ca.* 2 H, m), and 4.80 (*ca.* 1 H, m), [15-H_2 (**8**), (**9**), and (**10**) and 14-H_2 (**8**)], 1.74 and 1.68 [3 H, 2 × br s, 14-H_3 (**9**) and (**10**)], 0.98 and 1.00 (6 H, 2 × br s, 12-and 13-H_3); ^{13}C-{^{1}H} decoupled spectrum, many peaks, 70—160 p.p.m. region indicates four different types of exomethylenes and two endocyclic double bonds; $\nu_{max.}$ (KBr disc) 3 080 (=CH_2), 2 960, 2 940, and 2 860 (C-H), 1 635 (broad), and 900 (broad) (exocyclic C=CH_2), 1 550 (broad) and 1 370 (broad) (R-NO_2), 1 520 cm^{-1} (C=C-NO_2); *m/z* 249, 232, 219, 203, and 202.

The component R_F 0.67, 20% of the total photolysis products, is a clear oil. ^{1}H and ^{13}C n.m.r., i.r., and mass spectra show that this compound is isocaryophyllene (4,11,11-trimethyl-8-methylenebicyclo[7.2.0]-*cis*-undec-4-ene), (**6**), δ_H ($CDCl_3$) 5.20 (1 H, m, X of ABX system, $J_{AX} + J_{BX}$ 14 Hz, 5-H), 4.82 and 4.72 (2 H, AB quartet, *J* 2 Hz, 15-H_2), 2.55 (1 H, q, $J_{9,1} = J_{9,10} = 9$ Hz, 9-H), 1.7—2.4 (7 H, m, 1-H, 3-H_2, 6-H_2, and 7-H_2), 1.2—1.7 (4 H, m, 2-H_2 and 10-H_2), 1.65 (3 H, 14-H_3), 0.97 and 0.99 (6 H, 2 × s, 12-H_3 and 13-H_3); ^{13}C-{^{1}H} decoupled spectrum 51.89(d, C-1), 25.58(t, C-2), 28.91(t, C-3), 136.15(s, C-4), 124.93(d, C-5), 28.41(t, C-6), 35.51(t, C-7), 156.55(s, C-8), 40.09(d, C-9), 40.46(t, C-10), 33.06(s, C-11), 23.03(q, C-12), 29.94(q, C-13), 23.19(q, C-14), 110.34(t, C-15); $\nu_{max.}$ (thin film) 3 068 [=C(15)-H_2], 3 020 [=C(5)-H], 2 980, 2 960, and 2 860 (C-H), 1 670, 1 632, 885, and 875 (2 × C=C), 1 380, and 1 370 cm^{-1} (>CMe_2); *m/z* 204, 190, 189, and 174.

Acknowledgements

We wish to acknowledge our gratitude to the Carnegie Trust for the Universities of Scotland for a Research Scholarship (to D. K. MacA.), to the S.E.R.C. for a Research Scholarship (to J. A. P.), and to the S.E.R.C. for *X*-ray and e.p.r. equipment.

References

1 J. M. Robertson, 'International Review of Science, Series 2, Physical Chemistry, Chemical Crystallography,' Butterworths, London, 1975, vol. 11, p. 57, and references cited therein.
2 D. H. R. Barton and A. S. Lindsey, *J. Chem. Soc.*, 1951, 2988.
3 D. H. R. Barton, T. Bruun, and A. S. Lindsey, *J. Chem. Soc.*, 1952, 2210.
4 A. Aebi, D. H. R. Barton, and A. S. Lindsey, *J. Chem. Soc.*, 1953, 3124.
5 A. Aebi, D. H. R. Barton, A. W. Burgstahler, and A. S. Lindsey, *J. Chem. Soc.*, 1954, 4659.
6 F. Sörm, L. Dolejš, and J. Pliva, *Collect. Czech. Chem. Commun.*, 1950, **15**, 186.
7 F. Sörm, V. Jarolim, M. Streibl, and L. Dolejš, *Chem. Ind. (London)*, 1956, 154.
8 D. H. R. Barton and A. Nickon, *J. Chem. Soc.*, 1954, 4665.
9 E. J. Corey, R. B. Mitra, and H. Uda, *J. Am. Chem. Soc.*, 1964, **86**, 485.
10 D. M. Hawley, J. S. Roberts, G. Ferguson, and A. L. Porte, *Chem. Commun.*, 1967, 942.
11 D. M. Hawley, G. Ferguson, and J. M. Robertson, *J. Chem. Soc. B*, 1968, 1255.
12 O. Schreiner and C. F. James, *Pharm. Arch.*, 1898, **1**, 213.
13 O. Schreiner and E. Kremers, *Pharm. Arch.*, 1899, **2**, 14.
14 O. Schreiner and E. Kremers, *Pharm. Arch.*, 1899, **2**, 273.
15 O. Schreiner, *Pharm. Arch.*, 1903, **6**, 130.
16 E. Deussen, *Justus Liebig's Ann. Chem.*, 1909, **369**, 44.
17 E. Deussen, *Justus Liebig's Ann. Chem.*, 1912, **388**, 139.
18 E. Deussen, *J. Prakt. Chem.*, 1926, **114**, 63, and references cited therein.
19 P. Valenzuela and F. Daniels, *Philipp. J. Sci.* 1927, **34**, 187.
20 S. Mitchell, *J. Chem. Soc.*, 1928, 3258.
21 S. Mitchell, *J. Chem. Soc.*, 1930, 1829.
22 R. M. Hoffman, *J. Am. Chem. Soc.*, 1934, **56**, 1894.
23 A. A. McConnell, S. Mitchell, A. L. Porte, J. S. Roberts, and C. Thomson, *J. Chem. Soc. B*, 1970, 833.
24 P. Main, S. J. Fiske, G. Germain, S. E. Hull, J.-P. Declercq, L. Lessinger, and M. M. Woolfson, MULTAN-80, A System of Computer Programs for the Automatic Solution of Crystal Structures from *X*-ray Diffraction Data, Universities of York and Louvain, Belgium, 1980.
25 C. J. Gilmore, *J. Appl. Crystallogr.*, 1984, **17**, 42.
26 S. E. Hull and M. J. Irwin, *Acta Crystallogr.*, 1978, **A34**, 863.
27 W. B. Motherwell and J. S. Roberts, *J. Chem. Soc., Chem. Commun.*, 1972, 329.
28 O. H. Griffith, D. W. Cornell, and H. M. McConnell, *J. Chem. Phys.*, 1965, **43**, 2909.
29 O. H. Griffith and A. S. Waggoner, *Acc. Chem. Res.*, 1969, **2**, 17.
30 O. Kikuchi, *Bull. Chem. Soc. Jpn.*, 1969, **42**, 1187.
31 G. T. Knight and B. Pepper, *Tetrahedron*, 1971, **27**, 6201.
32 D. Mulvey and W. A. Waters, *J. Chem. Soc., Perkin Trans. 2*, 1978, 1059.
33 F. K. Kneubuhl, *J. Chem. Phys.*, 1960, **33**, 1074.

Received 25th July 1984; *Paper* 4/1301